

Three dimensional configuration of the secretory pathway and segregation of secretion granules in the yeast *Saccharomyces cerevisiae*

Alain Rambourg¹, Catherine L. Jackson^{2,*} and Yves Clermont³

¹Département de Biologie Cellulaire et Moléculaire, CEA/Saclay, F-91191 Gif-sur-Yvette, France

²Cell Biology and Metabolism Branch, NICHD, NIH, Bldg. 18T, Room 101, 18 Library Drive, Bethesda, MD 20892-5430, USA

³Department of Anatomy and Cell Biology, McGill University, 3640 University Street, Montréal, Québec, H3A 2B2, Canada

*Author for correspondence (e-mail: cathyj@helix.nih.gov)

Accepted 3 March 2001

Journal of Cell Science 114, 2231-2239 (2001) © The Company of Biologists Ltd

SUMMARY

The structural elements of the secretory pathway in the budding yeast *Saccharomyces cerevisiae* were analyzed by 3D stereo-electron microscopy using relatively thick sections in which membranes were selectively impregnated. In a wild-type strain, tubular networks of various sizes and staining properties were distributed throughout the cytoplasm. As a rule, wide-meshed, lightly stained polygonal networks were connected to more or less fenestrated sheets of endoplasmic reticulum (ER). Some of these networks were continuous with more intensely stained networks and narrower meshes that displayed at their intersections nodular dilations that progressively increased in size and staining properties to reach those of secretion granules. Such networks presumably corresponded to Golgi elements. Indeed, stacked cisternae typical of the mammalian Golgi apparatus are rarely found in wild-type cells. However, if it is assumed that the Golgi apparatus plays a key role in the segregation and maturation of secretion granules, then tubular networks with nodular dilations should be equivalent to parts of this organelle. In correlation with the increase in size and density of the nodules there was a decrease in diameter and staining intensity of the interconnecting tubules. These results parallel observations on the formation of secretory

granules in mammalian cells and suggest that the segregation of secretory material is concomitant with the progressive perforation and tubulization of previously unperforated sheets. When the *sec21-3* thermosensitive mutant was examined at the nonpermissive temperature (37°C), the secretory pathway was blocked at exit from the ER, which started to accumulate as clusters of narrow, anastomosed, unperforated ribbon-like elements. When the block was released by shifting down to permissive temperature (24°C), tubular networks of various sizes and caliber, presumably Golgi in nature, formed as soon as 5 minutes after release of the block. At later time intervals, granules of various sizes and densities appeared to be released by rupture of these tubular networks or even to form at the edges of ER fenestrae. These observations support a dynamic maturation process in which the formation of secretion granules occurs by means of an oriented series of membrane transformations starting at the ER and culminating with the liberation of secretion granules from Golgi networks.

Key words: Secretory pathway, Golgi apparatus, Secretion granules, Yeast, Brefeldin A, BFA, Trafficking

INTRODUCTION

Biochemical and genetic studies have made use of the yeast *Saccharomyces cerevisiae* to investigate cell biological processes and, in particular, those related to the secretory pathway. Temperature-sensitive secretion (*sec*) mutants have been shown to block protein traffic at various points along the secretory pathway and to accumulate secretory proteins within the endoplasmic reticulum (ER), Golgi apparatus or secretory granules (Schekman, 1992). Yet, as already indicated by Preuss et al., the scanty ER, the small size of Golgi units and the lack of appropriate staining methods for electron microscopy have hindered an adequate correlation of biochemical and structural data (Preuss et al., 1992). Using antibodies directed against Golgi marker proteins on negatively-stained thin sections, Preuss et al. identified Golgi-equivalent structures as a set of

isolated membranous elements surrounded by small vesicles. Rambourg et al., investigating thick sections in which membranes were selectively stained by reduced osmium and counterstained with lead, described small tubular networks interspersed throughout the cell that appeared independent from each other (Rambourg et al., 1993). Since some of these networks contained dilations with sizes and staining properties similar to those of secretory granules or vesicles, it was concluded that such structures might correspond to Golgi elements. In contrast to most techniques previously used for studying yeast cells by electron microscopy, reduced osmium not only delineated membranes but also stained the content of ER cisternae, Golgi-like elements and secretion granules, thus facilitating their identification and examination in three dimensions. Furthermore, the staining gradient increased from the nuclear envelope to the secretion granules and cell wall.

This observation suggested that reducing substances such as carbohydrates, known to be progressively added to proteins along the secretory pathway, were responsible for the staining of the content of cell organelles involved in secretion (Rambourg et al., 1993). Using this method, the nuclear envelope and ER cisternae were only lightly stained and hence barely delineated against the cytoplasmic background. This drawback can be overcome by counterstaining osmium-reduced sections with thiocarbohydrazide rather than lead. Under these conditions, the staining of the cisternal and tubular elements of the ER is significantly increased and hence greatly facilitates their identification. It is the purpose of the present study to re-examine, with this more sensitive method the structural configuration of the elements of the secretory pathway in a wild-type strain of *S. cerevisiae*. Furthermore, to clarify the spatio-temporal relationship between these structures and the ER, their modifications have been studied using specific blocks at early stages of the secretory pathway. First, we examined the modifications introduced by a short treatment with brefeldin A (BFA), the effects of which on transport have been well-studied (Brigance et al., 2000; Graham et al., 1993). In addition, the temperature-sensitive mutant *sec21-3*, which blocks ER-Golgi transport (Gaynor and Emr, 1997), was examined at restrictive temperature and after return to permissive temperature for various lengths of time.

MATERIALS AND METHODS

Yeast strains used in this study were CJY049-3-4 MAT α ura3-52 leu2-3,112 his3- Δ 200 lys2-801 ade2-101, CJY004 MAT α ura3-52 erg6- Δ 1 and EGY0213 MAT α ura3-52 leu2-3,112 his3- Δ 200 trp1- Δ 901 suc2 Δ 9 sec21::HIS3/ p315sec21-3 (LEU2 CEN6 sec21-3) (Gaynor and Emr, 1997). Strains were grown in liquid YPD medium (2% Bacto-peptone (w/v), 1% yeast extract (w/v) and 2% glucose (w/v)). Cultures were grown to an OD₆₀₀ of 0.2-0.5 at 24°C in a shaking water bath. Cells were centrifuged, resuspended in a small volume of YPD, then injected into 50 ml of prewarmed YPD medium in a 37°C shaking water bath. Wild-type cells were maintained for 40 minutes at 37°C. Mutants were maintained at 37°C for 20 minutes, then either fixed immediately or transferred to a 24°C water bath for 5, 10 or 20 minutes before fixation.

Cell fixation was initiated by adding 1 ml of 20% glutaraldehyde directly to the cultures (final concentration 0.5%), and flasks were left in the shaking water bath for at least 5 minutes. Cells were then harvested, resuspended in fixative containing 2% glutaraldehyde in 0.1 M cocodylate buffer, pH 6.8, 1 M sorbitol, and left overnight at 4°C.

Cells were transferred for 15 minutes at room temperature in 1% sodium metaperiodate and then postfixed for 1 hour at room temperature in a 1:1 mixture of 2% aqueous osmium tetroxide and 3% aqueous potassium ferrocyanide (Karnovsky, 1971). Dehydration was carried out in ethanol followed by embedding in Epon. 200 nm thick sections were cut with a Reichert automatic ultramicrotome and counterstained with a technique derived from the thiocarbohydrazide-silver proteinate method previously described (Thiéry and Rambourg, 1974). Sections placed on nickel grids were floated for 10 minutes at room temperature on a 1% aqueous solution of thiocarbohydrazide in 10% acetic acid. After several rinses in acetic acid solutions of decreasing concentrations, they were transferred on distilled water, stained for 10 minutes on a 1% aqueous solution of silver proteinate and carefully rinsed in distilled water. They were then examined with a CM 12 Philips electron microscope at 80 kV.

For stereoscopy, grids were placed on the goniometric stage of the

electron microscope, and stereopairs were obtained by taking pictures of the same field after tilting the specimen at -10° and $+10^\circ$ from the 0° position. A 3D image of the structures was then obtained by looking at properly adjusted pairs of such photographs with anaglyph (red/blue) glasses, the red lens being placed over the left eye. 68 stereopairs of wild-type cells were examined. A rough estimation indicated that 97% of images contained tubular networks and granules of various sizes. 49% of images displayed wide-meshed lightly stained networks as opposed to 84% of specimens with darkly stained tubular networks with narrower meshes and nodular dilations.

RESULTS

Stained membrane structures in a wild-type strain

In wild-type cells grown at 24°C or 37°C, the nucleus was delimited by a well delineated nuclear envelope perforated by nuclear pores (Fig. 1a,b). This nuclear envelope was continuous with stained sheets and ribbons that extended into the surrounding cytoplasm, and occasionally could be seen to establish links with more or less perforated sheets located at the cell periphery, just beneath the plasma membrane. In the past, such structures have been considered as elements of the ER and will continue to be considered as such in the following description (Rambourg et al., 1993).

Any of these ER elements could display continuities with membranous tubules forming networks of various sizes and staining densities (Fig. 1a; Fig. 2a). Some of these networks showed approximately the same staining intensity as the more or less perforated sheets to which they were connected (Fig. 1c; Fig. 2a). They were wide-meshed and often connected to networks with narrower meshes that showed at their intersections nodular dilations of increasing size and staining intensity (Fig. 2b,d). Large strongly stained dilations were similar in size and staining intensity to secretion granules seen throughout the cytoplasm (Fig. 1a,b; Fig. 2d,e) and clustering within the growing bud (Fig. 2f). Strings of strongly stained granules were observed in proximity to the tubular networks (Fig. 1c). Occasionally, in such strings of granules, the interconnecting areas between two adjacent dilations were barely stained and seemed to be deprived of any reactive content (Fig. 2e). In buds, strongly stained granules were at times interconnected by more or less reactive tubular bridges (Fig. 2f, arrow).

In addition to tubular networks, other membrane-bound structures were observed. They usually appeared as poorly fenestrated spheres in continuity with the subplasmalemmal ER (Fig. 3a), the nuclear envelope (Fig. 3b) or with poorly perforated ER elements in the cytoplasm (Fig. 3c). They were more numerous in wild-type strains grown at 37°C than at 24°C and their staining intensity varied from that of the nuclear envelope or ribbons to which they were associated (Fig. 3c), to the strong staining intensity of the vacuole (Fig. 3b).

Stained membrane structures in *erg6* strains treated with BFA

As early as 5 minutes after adding BFA, strongly stained secretion granules disappeared from the cytoplasm (Fig. 4) and were absent from buds. ER elements did not differ significantly from those observed in untreated strains. They showed,

however, a tendency to fold upon themselves to form cylinders (Fig. 4a) and spheres (Fig. 4b). Such spheres were sometimes interconnected and resembled, by their size and staining properties, the strongly stained vacuole (Fig. 4b). As in wild-type strains, non-perforated sheets were continuous with wide-meshed tubular networks that occasionally showed small, intensely stained nodules at intersections of the anastomosed tubules (Fig. 4a,d). Other networks made up of thinner tubules with narrower meshes formed, in contrast to those observed in wild-type strains, large multilayered ovoid or spherical masses (Fig. 4c) and parallel arrays (Figs 4d,e). In both types of structures, more intensely stained nodules were present at the intersections of the narrow meshes of the networks (Fig. 4c,d).

Stained membrane structures in *sec21-3*

When the *sec21-3* mutant was incubated for 5 minutes at the restrictive temperature (37°C), the non-perforated ER elements extending from the nuclear envelope remained unaffected (Fig. 5a). Within the cytoplasm, tubular fragments in which large, strongly stained nodules were interconnected by less reactive areas were frequently observed (Fig. 5a). Ovoid masses of tightly anastomosed membranes were frequently encountered in close contact with the nuclear envelope (Fig. 5a). These membranes consisted mainly of narrow ribbon-like and unperforated elements.

After 20 minutes at 37°C, the tubular fragments were no longer visible, whereas extensive masses of anastomosed ribbon-like elements formed bridges between the nuclear envelope and the poorly perforated sheets underlying the plasma membrane (Fig. 5b).

As early as 5 minutes after returning the mutant to

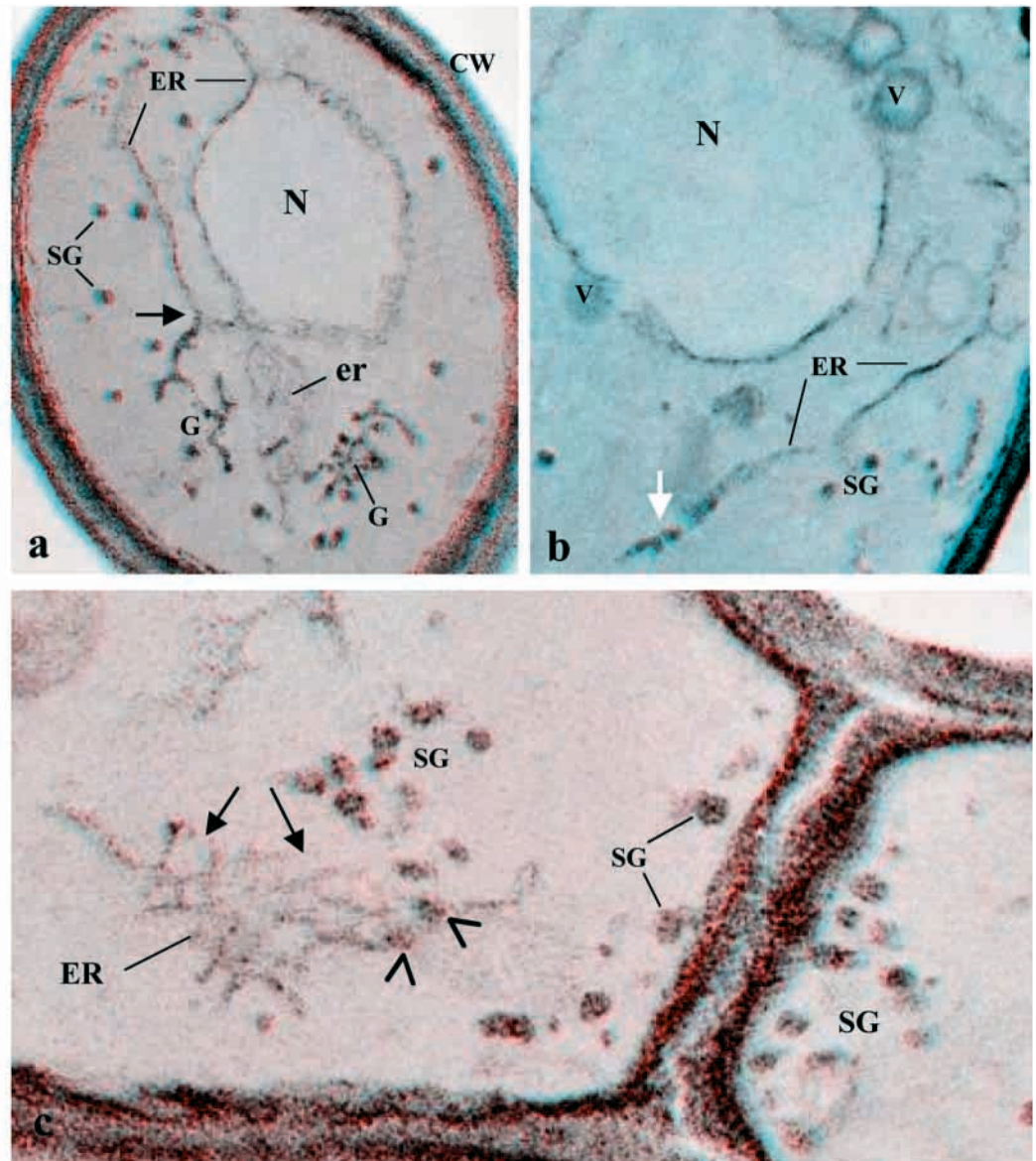
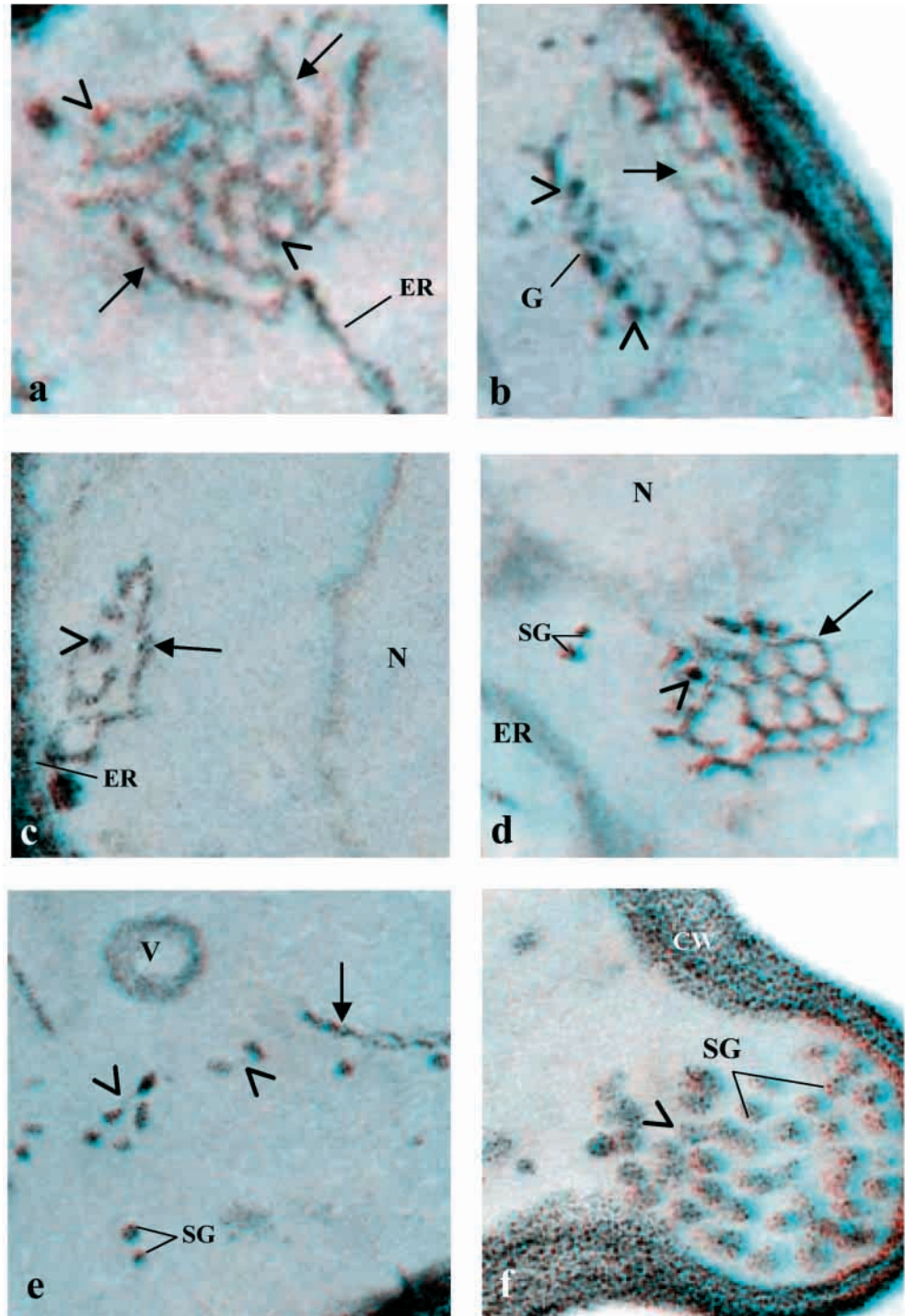


Fig. 1. Three stereopairs of 0.20 μm thick sections of wild-type *S. cerevisiae* cells grown at 24°C. (a) Shows a nucleus (N) delimited by a lightly stained nuclear envelope in continuity with ER sheets or ribbons seen in side view (ER). One of these ER elements is continuous (arrow) with a strongly stained tubular network, probably a Golgi element (G). Another sheet of ER seen in face view (er) is in close proximity to another strongly stained tubular network showing more intensely stained nodular dilations (G). Intensely stained free secretion granules (SG) are interspersed throughout the cytoplasm. CW, cell wall. Magnification $\times 18,800$. (b) Lightly stained ER ribbons are seen in oblique or side views (ER). Strongly stained structures resembling secretion granules (white arrow) are observed at the left-hand extremity of an obliquely sectioned ER ribbon. Spherical membranous structures (V) resembling vacuoles are in close contact with the nuclear envelope. N, nucleus. Magnification $\times 40,500$. (c) A non-perforated ER sheet (ER) seen in face view is continuous at its periphery with lightly stained anastomosed tubules (arrows) forming a wide-meshed tubular network. At the right-hand side extremity of this network, there are more intensely stained dilations (arrowheads) that resemble secretion granules (SG). Magnification $\times 74,000$.

permissive temperature, oval fenestrae (Fig. 5c) and polygonal arrays of membranous tubules (Fig. 5c,d) were seen at the periphery of nonperforated ER sheets. Dilations reappeared at the intersections of the anastomosed tubules (Fig. 5c,d). After 10 minutes, numerous, more or less fragmented tubular networks with dilations of various size and density were

Fig. 2. Tubular networks and secretion granules in 0.20 μm thick sections of wild-type *S. cerevisiae* cells. (a) A wide-meshed tubular network (arrows) is connected to an ER ribbon seen in side view (ER). Nodular dilations of variable staining are shown at arrowheads. Magnification $\times 70,000$. (b) A wide-meshed lightly stained tubular network (arrow) is seen just below the cell wall. Heavily stained dilations (arrowheads) are present at the intersections of tubules making up a Golgi network with narrower polygonal meshes (G). CW, cell wall. Magnification $\times 66,800$. (c) A tubular network (arrow) with dilations (arrowhead) is observed next to the subplasmalemmal ER (ER). The nucleus (N) is delimited by the lightly stained nuclear envelope. Magnification $\times 72,600$. (d) A wide-meshed tubular network (arrow) with an intensely stained dilation (arrowhead) is adjacent to the nucleus (N). ER, ER ribbon; SG, free secretion granules. Magnification $\times 32,200$. (e) Next to a tubular network (vertical arrow) seen side view there are secretion granules bridged by thin faintly stained tubules (arrowheads). A portion of the strongly reactive cell wall is seen at the bottom-right. V, small vacuole-like structure. Magnification $\times 36,300$. (f) Numerous secretion granules (SG) are clustered in the bud of a growing cell. Several granules are still connected (arrowhead). The cell wall is strongly stained (CW). Magnification $\times 81,100$.



interspersed throughout the cytoplasm (Fig. 5f). Occasionally, dilations similar to mature secretion granules were present at the edges of ER fenestrae (Fig. 5e). Secretion granules were numerous at this time; they were dispersed throughout the cytoplasm (Fig. 5e,f) but sometimes, as in wild-type cells, accumulated in the bud (Fig. 5e). Small vesicles were never observed and vacuole-like structures were rarely encountered along ER elements. Vacuole-like structures appeared instead to accumulate in large, intensely stained vacuoles or in their immediate vicinity (Fig. 5g).

DISCUSSION

Membranous tubules and segregation of secretion granules

In animal or plant cells in which the Golgi apparatus consists of isolated or interconnected stacks of saccules (Farquhar, 1985; Farquhar and Palade, 1981), secretion granules are thought to bud from the edges of the trans-most saccule. Yet, when the Golgi apparatus of several types of rat glandular cells was examined in three dimensions in relatively thick sections

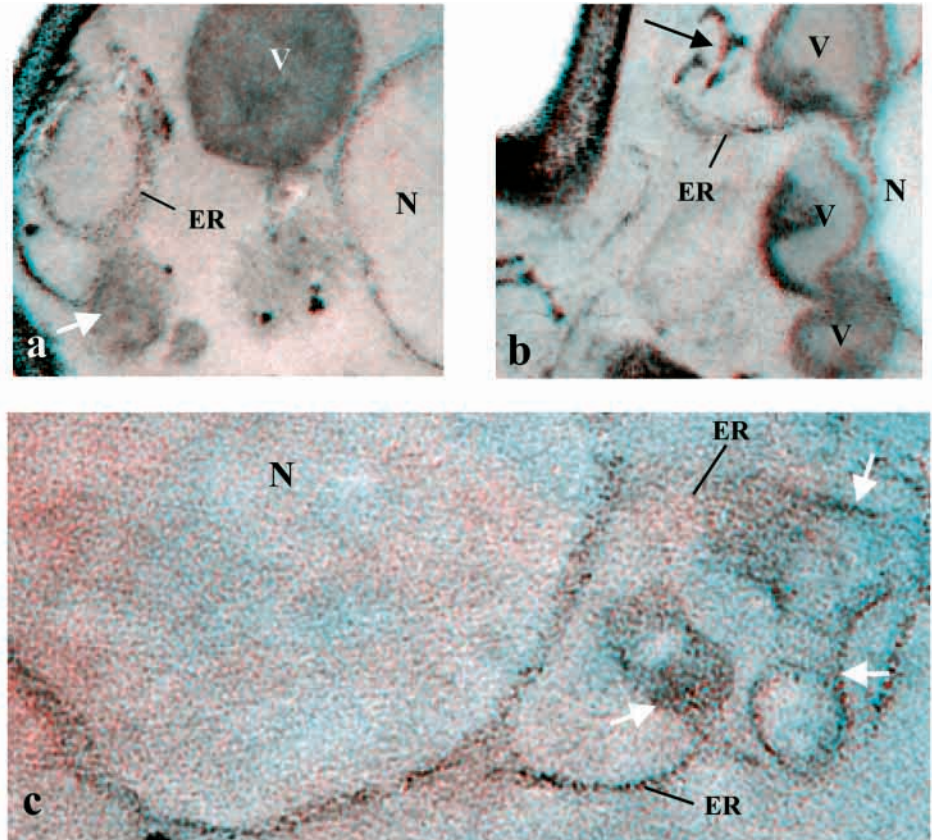


Fig. 3. Spherical and cylindrical structures in 0.20 μm thick sections of wild-type *S. cerevisiae* cells grown at 37°C. (a) A poorly perforated sheet of endoplasmic reticulum curves (ER) and forms a cylindrical structure (white arrow). A large, well-stained vacuole (V) is located adjacent to the nucleus (N). Magnification $\times 38,500$. (b) Three vacuole-like spherical structures (V) are connected to the nuclear envelope (N). The vacuole structure at the top-right is continuous with a sheet of unperforated ER (ER). A tubular network (arrow) is also labeled. Magnification $\times 52,400$. (c) Connected to the nuclear envelope, an unperforated ER sheet (ER) forms cylindrical structures (arrows). N, nucleus. Magnification $\times 67,400$.

(Clermont et al., 1992; Rambourg et al., 1987), the secretion granules seemed to form in the following manner: the secretory material first appears to be evenly distributed along the continuous and poorly fenestrated elements making up the so-called mid-compartment. Then the saccular elements located on the trans aspect of these poorly fenestrated elements become more fenestrated, while the secretory material accumulates in nodular swellings separated by highly perforated or tubular portions. In the trans-most Golgi elements, the nodular swellings reach their final size and remain interconnected by flattened anastomosed membranous-tubules. At some distance from the Golgi saccules, small shriveled residual tubular networks are interspersed among free prosecretory granules that progressively transform into denser, mature secretion granules. In yeasts, as shown in the present study, nodular swellings resembling secretion granules are encountered at the intersections of polygonal meshes made up by interconnected membranous tubules or at the edges of oval fenestrae located at the periphery of poorly perforated sheets. In contrast to tubular areas located proximal to unperforated sheets that make up the nuclear envelope or membranous elements underlying the cell surface, the tubular portions that interconnect strongly stained and seemingly fully developed nodular swellings are frequently deprived of stained material, while free secretion granules are present in their immediate surroundings. Thus, it is likely that, in yeast as in mammalian cells (Rambourg and Clermont, 1990; Rambourg and Clermont, 1997), the liberation of secretion granules occurs by rupture of tubular areas and not by budding from the edges of saccular elements. As in mammalian cells, the segregation of secretory material appears

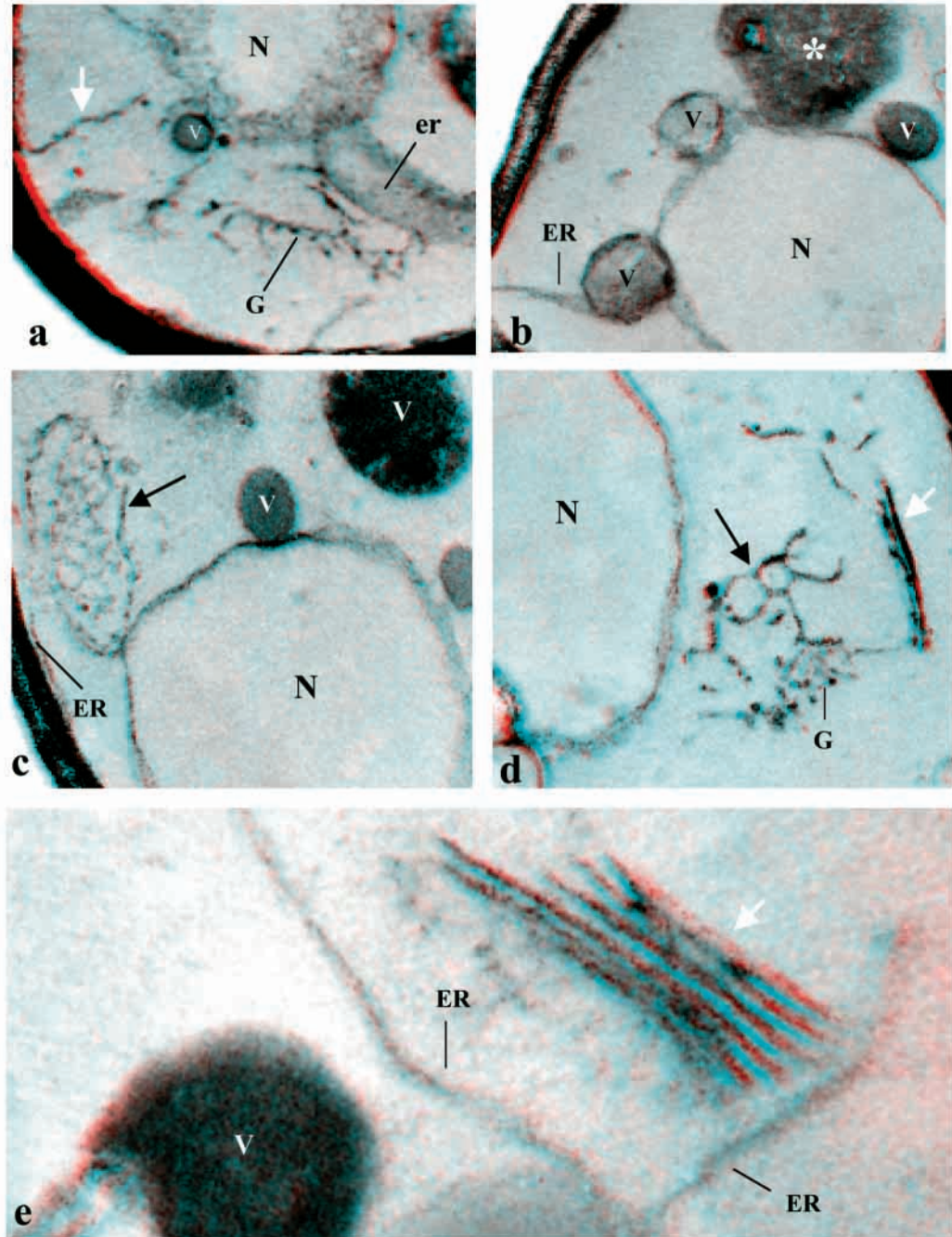
to be concomitant with the progressive perforation and tubulization of previously unperforated sheets.

Structure of the Golgi apparatus in *S. cerevisiae*

It is generally assumed that in yeasts, as in mammalian cells, the Golgi apparatus consists of independent stacks of saccules interspersed throughout the cytoplasm (Pelham, 1998). Indeed, Golgi stacks consisting of several closely opposed parallel saccules are observed in the yeasts *Schizosaccharomyces pombe* (Chappell and Warren, 1989) and *Pichia pastoris* (Rambourg et al., 1995b; Rossanese et al., 1999). However, stacked cisternae are rarely found in wild-type cells of *S. cerevisiae* (Duden and Schekman, 1997; Rambourg et al., 1995b). Immuno-EM studies have shown that in *S. cerevisiae*, Golgi markers are localized in single 'banana-like' cisternae (Preuss et al., 1992). However, their small size and the difficulty in obtaining a good contrast under the conditions required for immunological analysis makes it difficult to accurately visualize their ultrastructural characteristics. Previous studies using stereo-electron microscopy (Rambourg et al., 1993) have failed to identify isolated cisternae, but have instead revealed tubular networks (Rambourg et al., 1995b). Several lines of evidence support the conclusion that at least some of these tubular networks correspond to Golgi elements.

When mutants *sec18* and *sec23*, which block transport of proteins from the ER to the Golgi, were incubated at the nonpermissive temperature, tubular networks disappeared. When these mutants were then returned to the permissive temperature, tubular networks reappeared (Morin-Ganet et al., 1998; Morin-Ganet et al., 2000).

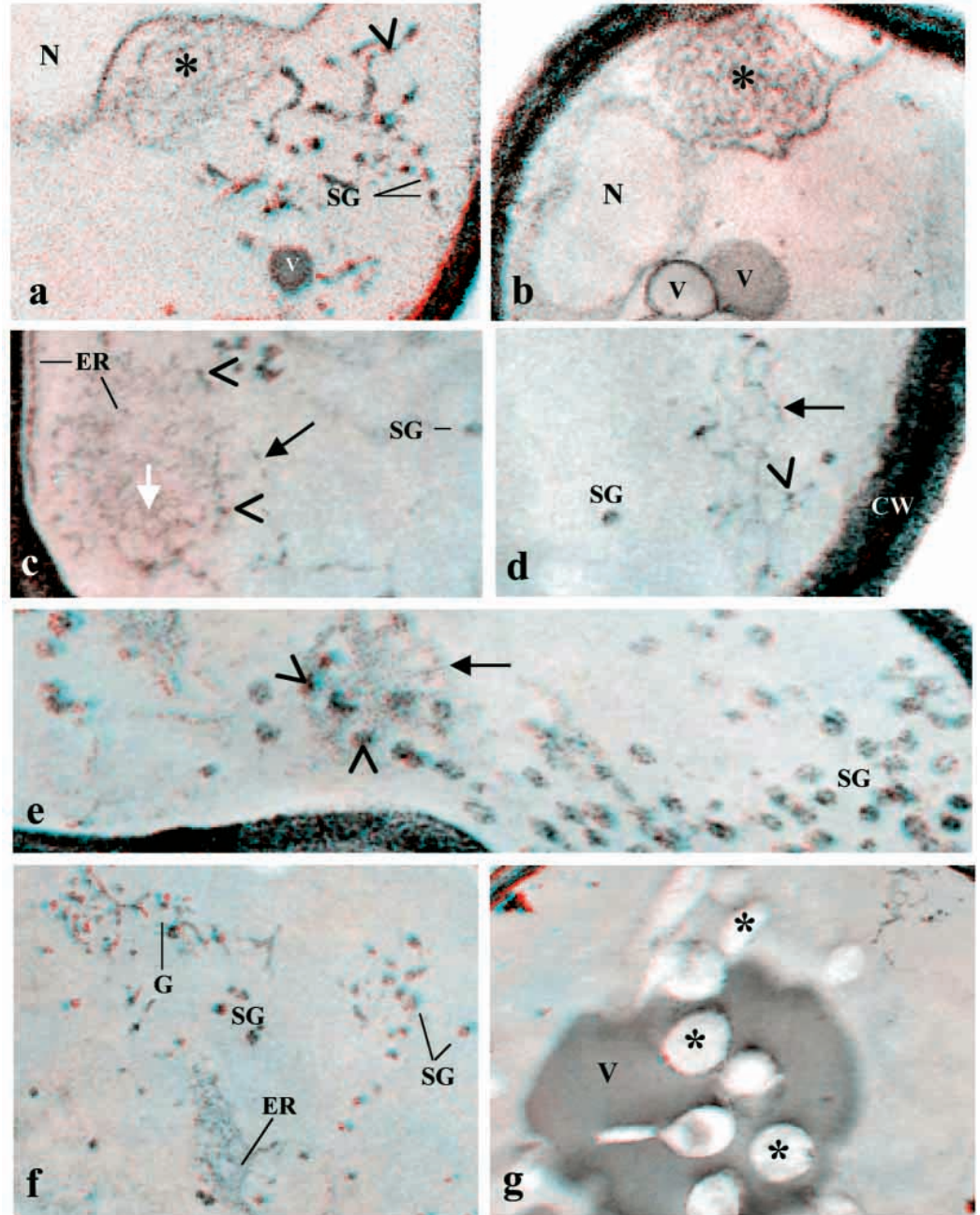
Fig. 4. *erg6* strain treated for 5 minutes with BFA. (a) A tubular Golgi network with small dilations at the intersections of polygonal meshes (G) is seen next to a curved sheet of unperforated ER (er). At the left, a tubular network (white arrow) is seen in profile and is continuous with a portion of subplasmalemmal ER at the top-left. A small vacuole-like structure (V) is located next to the nucleus (N). Magnification $\times 39,700$. (b) Several small vacuole-like structures of variable staining densities (V) are in close contact with the nuclear envelope. At the bottom-left, one of these structures is continuous with an ER sheet (ER). A large intensely stained vacuole (*) is seen proximal to the nucleus (N). Magnification $\times 38,500$. (c) Next to the nucleus (N) and connected to a subplasmalemmal ER sheet (ER), there is a large tubular network (arrow) forming an ovoid mass. Light and dense vacuoles are also labeled (V). Magnification $\times 40,100$. (d) A tubular Golgi network with small dilations at the intersections of narrow, irregular meshes (G) is continuous at one side with a wide-meshed tubular network (arrow) and is connected on the right with a parallel array of anastomosed tubules (white arrow). N, nucleus. Magnification $\times 43,350$. (e) A parallel array of saccules (white arrow) is seen in proximity to an ER sheet (ER). A large vacuole is labeled (V). Magnification $\times 82,100$.



Treatment of cells with BFA for short time intervals leads to accumulation of tubular networks giving rise to large ovoid or spherical structures that are connected to the ER (Fig. 4; Rambourg et al., 1995a). Analysis of ER-Golgi transport of marker proteins such as alpha factor has shown that BFA blocks two biochemically defined steps of transport: ER-Golgi and an early Golgi step (Brigance et al., 2000; Graham et al., 1993). When BFA-treated cells were examined by immunofluorescence, the cis-Golgi marker Och1p was found in spots somewhat larger than those seen in untreated cells, indicating that the cis-Golgi does not disappear at early time points after BFA addition (data not shown). These results strongly support the conclusion that tubular networks that accumulate in BFA-treated cells correspond to the yeast cis-

Golgi. In BFA-treated cells, networks containing strongly stained nodules that resemble secretion granules were not observed. When *sec18* and *sec23* mutants maintained at the restrictive temperature were then returned to the permissive temperature, such networks reappeared later than the cis-Golgi tubular networks (Morin-Ganet et al., 1998; Morin-Ganet et al., 2000). They would thus correspond to the trans-tubular parts of the Golgi apparatus in mammalian cells which, in secretory cells, are known to break to liberate prosecretory granules into the surrounding cytoplasm (Rambourg and Clermont, 1990; Rambourg and Clermont, 1997). Finally, as shown in the accompanying article (Peyroche et al., 2001), the *geal-4* mutant defective in ER-Golgi transport, accumulated large ring-like structures

Fig. 5. *sec21-3* mutant maintained for 5 minutes (a) and 20 minutes (b) at 37°C, blocked for 20 minutes at 37°C and returned for 5 (c,d) or 10 minutes (e,f,g) to permissive temperature (24°C). (a) After 5 minutes at 37°C, tubular fragments with nodular dilations (arrowhead) are interspersed within the cytoplasm. An ovoid mass made up of interconnected short ribbon-like ER elements (*) is continuous with the nuclear envelope. V, small vacuole; N, nucleus; SG, free secretion granules. Magnification $\times 40,800$. (b) After 20 minutes at 37°C, the secretion granules and tubular fragments with or without dilations are no longer seen. A mass of interconnected ribbon-like ER elements (*) forms a bridge between the nuclear envelope and the subplasmalemmal ER at the top-right. Two vacuole-like structures (V) are present next to the nucleus (N). Magnification $\times 35,400$. (c) As early as 5 minutes after shifting the temperature down to 24°C, fenestrations (white arrow) and tubular networks (arrow) with dilations (arrowheads) are seen at the periphery of an unperforated sheet of ER, which is itself continuous with the subplasmalemmal ER (ER). Magnification $\times 42,000$. (d) After 5 minutes at 24°C, a tubular network (arrow) with more intensely stained dilations (arrowhead) is observed. SG, a free secretion granule; CW, cell wall. Magnification $\times 48,000$. (e) At 10 minutes after shifting the cells back to 24°C, numerous secretion granules (SG) are interspersed within the cytoplasm and accumulate in the bud on the right. At the center left, an ER sheet seen in face view shows peripheral tubules (arrow) and dilations (arrowheads) with size and staining properties similar to those of secretion granules. Magnification $\times 59,100$. (f) After 10 minutes at 24°C, a broken tubular network, presumably a Golgi element (G), with dilations of various sizes and staining intensities is observed at the top-left. SG, free secretion granules; ER, an ER sheet with a fenestrated periphery. Magnification $\times 35,000$. (g) Small poorly contrasted vacuole-like structures (*) accumulate inside or in close proximity to a large intensely reactive vacuole (V). Magnification $\times 23,300$.



that contain the Golgi markers Och1p, Anp1p and Mnn1p. When examined by 3D electron microscopy, such ring-like structures consisted of tubular networks which, although larger in size, resembled those observed in wild-type cells.

It should be stressed, however, that in wild-type *S. cerevisiae* cells, the 3D organization of these networks varies considerably from one cell to another or even in the same cell; they may be scattered throughout the cytoplasm as independent

units. In addition, they might form a continuous structure in continuity at one end with unperforated poorly stained sheets, making up the subplasmalemmal ER or nuclear envelope, and at the other end give rise to intensely stained secretion granules. In some cases, these tubular networks seem to be lacking along the secretory pathway, as secretion granules may arise without any intervening structure from the perforated sheets at the extremities of the ER. The question then arises as to how these observations may be reconciled with the current models of

Golgi structure and function that are based on the concept of distinct, saccular cisternae.

'Vectorial' membrane flow within the secretory pathway

Until recently, the model widely accepted to explain the cis-trans or anterograde transport of proteins to and through the Golgi apparatus was the 'vesicular transport model' (Farquhar, 1985; Pelham, 1998; Rothman and Wieland, 1996). According to this model, vesicles budding from ER cisternae transport proteins and fuse with the cis-tubular network observed on the cis-face of the Golgi apparatus of most mammalian cells. Cargo proteins are then transported from the cis- to the trans-face of the Golgi stack by means of small vesicles located on its trans-aspect that bud from the edges of one saccule and fuse with the edges of the next one, until they reach the trans-compartment, where they are finally packaged within secretory granules and/or vesicles. According to such a scheme, the cis, mid and trans-compartments are considered as separate and stationary elements, in contrast to vesicles, which are transient and moving from one compartment to another.

According to an alternative model, the 'saccular migration model', (Mollenhauer and Morre, 1991) or the 'cisternal maturation model' (Glick and Malhotra, 1998; Pelham, 1998), saccular membrane and secretory products move and mature from the cis- to the trans-face of the Golgi apparatus, where they are released as secretory granules among vesicular and tubular remnants. Indeed, as shown in secretory epithelial cells of rat seminal vesicles (Clermont et al., 1992), the secretory granules contain an eccentric electron-dense spherical body with one pole attached to their delimiting membrane. The earliest stage of segregation of the precursor of this dense body is observed in dilations of the cis-tubular network. These dilations with the dense body still attached to their membrane increase in size along the cis-trans axis of the stacks. Then, on the trans-aspect of the Golgi stack, there is a rupture of the trans-most Golgi elements with a concomitant liberation of secretion granules. In non-glandular mammalian cells, there is a progressive fenestration of the saccules in the cis-trans direction, peeling off and rupture of sacculotubular elements on the trans-aspect of the Golgi apparatus (Rambourg and Clermont, 1990; Rambourg and Clermont, 1997). Thus, in all cells examined, including non-glandular cells, there is a loss of membrane on the trans-aspect of the Golgi apparatus. This loss of membrane, as postulated by Mollenhauer and Morré, has to be compensated by the addition of membrane on the cis-aspect of the Golgi apparatus accompanied by a flow of membrane in a cis-trans or anterograde direction (Mollenhauer and Morre, 1991).

In the yeast *S. cerevisiae*, stacks of saccules, at least in wild-type cells, are only rarely observed. The only situation in which Golgi saccules or cisternae have been clearly identified is in the thermosensitive *sec7-1* secretory mutant at the nonpermissive temperature. In addition, this situation provided the opportunity to understand how stacks of saccules develop from purely tubular Golgi networks. Indeed, when *sec7-1* was maintained for increasing amounts of time at the nonpermissive temperature of 37°C the secretion granules progressively decreased in number and soon disappeared. Concomitantly, the networks of Golgi tubules increased in size and complexity, lost their distensions (prosecretory granules)

and finally transformed into flattened saccules forming stacks of up to seven or eight saccules that were similar to the Golgi stacks in mammalian cells (Rambourg et al., 1993). As in spermatids (Clermont et al., 1994) and Sertoli cells (Rambourg et al., 1979), connections between the saccules were evident, but, in contrast to what was observed in the latter cells, Golgi-associated small vesicles were generally absent. Thus, in this particular case, no saccular migration or vesicular transfer was observed but rather the formation of saccules as the result of what appeared to be a continuous membrane flow.

When a *sec18* thermosensitive mutant was placed for 10 minutes at the nonpermissive temperature of 37°C, the Golgi tubular networks and secretory granules were no longer observed and small tubulovesicular fragments accumulated in the cytoplasm (Morin-Ganet et al., 1998; Morin-Ganet et al., 2000). When the block was released by shifting down to the permissive temperature of 25°C, isolated tubulovesicular fragments decreased in number and seemed to reassociate to form tubulovesicular clusters, while the first secretory granules started to be produced. Later on, tubular Golgi networks reappeared progressively with a concomitant disappearance of the tubulovesicular clusters. Finally, at later time intervals, secretory granules accumulated in the bud, the 3D configuration of Golgi networks was restored to that observed in wild-type cells and small vesicular or tubular fragments were rarely encountered in the cytoplasm. It was thus concluded that the yeast Golgi apparatus at steady state consists of a continuously renewed set of transitory membrane-bound structures, rather than a permanent cell organelle. The observations suggested that tubular networks are constantly renewed by fusion of vesiculotubular elements presumably originating from the ER (Morin-Ganet et al., 1998; Morin-Ganet et al., 2000).

If tubular networks arise from fusion of ER-derived vesicles, then intermediates in this process should be observed in wild-type cells. However, in the present study, isolated vesicles or tubules are rarely encountered in wild-type cells. Instead, tubular networks with dilations reminiscent of pro-secretory granules are frequently in structural continuity with the nuclear envelope or the subplasmalemmal ER. Furthermore, when the *sec21-3* thermosensitive mutant was placed for 20 minutes at the nonpermissive temperature of 37°C, the secretory pathway appeared to be blocked at the exit of the ER, which started to accumulate as clusters of anastomosed ribbon-like elements. When the block was released by shifting down to the permissive temperature, no vesicular or vesiculotubular fragments were ever observed. Tubular networks of various sizes and calibers formed as soon as 5 minutes after release of the block, while granules of various sizes and densities appeared to be released by rupture of these tubular networks or even to form at the edges of ER fenestrae.

These observations, as well as the large variability of structures observed from cell to cell or even within the same cell indicate that a series of fixed structural compartments is not a necessary prerequisite for cargo transport between the ER and secretory granules. They would instead support a dynamic maturation model in which vectorial membrane flow is directed through a defined series of membrane transformations starting at the ER, leading to formation of tubular networks and culminating with the liberation of secretion granules. The function of such structures would be the production of

secretory granules or vesicles through the progressive concentration of secretory cargo into nodes of the tubular networks and the subsequent fragmentation of the interconnecting tubules to liberate secretory granules or vesicles into the surrounding cytoplasm.

We thank Corinne Le Moal, CEA Saclay, for excellent technical assistance.

REFERENCES

- Brigance, W. T., Barlowe, C. and Graham, T. R.** (2000). Organization of the yeast Golgi complex into at least four functionally distinct compartments. *Mol. Biol. Cell* **11**, 171-182.
- Chappell, T. G. and Warren, G.** (1989). A galactosyltransferase from the fission yeast *Schizosaccharomyces pombe*. *J. Cell Biol.* **109**, 2693-2702.
- Clermont, Y., Rambourg, A. and Hermo, L.** (1992). Segregation of secretory material in all elements of the Golgi apparatus in principal epithelial cells of the rat seminal vesicle. *Anat. Rec.* **232**, 349-358.
- Clermont, Y., Rambourg, A. and Hermo, L.** (1994). Connections between the various elements of the *cis*- and *mid*-compartments of the Golgi apparatus of early rat spermatids. *Anat. Rec.* **240**, 469-480.
- Duden, R. and Schekman, R.** (1997). Insights into Golgi function through mutants in yeast and animal cells. In *The Golgi Apparatus*. (ed. E. G. Berger and J. Roth), pp. 219-246. Basel/Switzerland: Birkhäuser Verlag.
- Farquhar, M. G.** (1985). Progress in unraveling pathways of Golgi traffic. *Annu. Rev. Cell Biol.* **1**, 447-488.
- Farquhar, M. G. and Palade, G. E.** (1981). The Golgi apparatus (complex)-(1954-1981)-from artifact to center stage. *J. Cell Biol.* **91**, 77s-103s.
- Gaynor, E. C. and Emr, S. D.** (1997). COPI-independent anterograde transport: cargo-selective ER to Golgi protein transport in yeast COPI mutants. *J. Cell Biol.* **136**, 789-802.
- Glick, B. S. and Malhotra, V.** (1998). The curious status of the Golgi apparatus. *Cell* **95**, 883-889.
- Graham, T. R., Scott, P. A. and Emr, S. D.** (1993). Brefeldin A reversibly blocks early but not late protein transport steps in the yeast secretory pathway. *EMBO J.* **12**, 869-877.
- Karnovsky, M. J.** (1971). Use of ferrocyanide-reduced osmium tetroxide in electron microscopy. *American Society of Cell Biology* (11th Meeting) Abstr. **284**, 146.
- Mollenhauer, H. H. and Morre, D. J.** (1991). Perspectives on Golgi apparatus form and function. *J. Electron Microsc. Tech.* **17**, 2-14.
- Morin-Ganet, M. N., Rambourg, A., Clermont, Y. and Kepes, F.** (1998). Role of endoplasmic reticulum-derived vesicles in the formation of Golgi elements in *sec23* and *sec18* *Saccharomyces Cerevisiae* mutants. *Anat. Rec.* **251**, 256-264.
- Morin-Ganet, M. N., Rambourg, A., Deitz, S. B., Franzusoff, A. and Kepes, F.** (2000). Morphogenesis and dynamics of the yeast Golgi apparatus. *Traffic* **1**, 56-68.
- Pelham, H. R.** (1998). Getting through the Golgi complex. *Trends Cell Biol.* **8**, 45-9.
- Peyroche, A., Courbeyrette, R., Rambourg, A. and Jackson, C. L.** (2001). The ARF exchange factors *Gea1p* and *Gea2p* regulate Golgi structure and function in yeast. *J. Cell Sci.* **114**, 2241-2253.
- Preuss, D., Mulholland, J., Franzusoff, A., Segev, N. and Botstein, D.** (1992). Characterization of the *Saccharomyces* Golgi complex through the cell cycle by immunoelectron microscopy. *Mol. Biol. Cell* **3**, 789-803.
- Rambourg, A. and Clermont, Y.** (1997). Three-dimensional structure of the Golgi apparatus in mammalian cells. In *The Golgi Apparatus*. (ed. E. G. Berger and J. Roth), pp. 37-61. Basel, Switzerland: Birkhäuser Verlag.
- Rambourg, A. and Clermont, Y.** (1990). Three-dimensional electron microscopy: structure of the Golgi apparatus. *Eur. J. Cell Biol.* **51**, 189-200.
- Rambourg, A., Clermont, Y. and Hermo, L.** (1979). Three-dimensional architecture of the golgi apparatus in Sertoli cells of the rat. *Am. J. Anat.* **154**, 455-476.
- Rambourg, A., Clermont, Y., Hermo, L. and Segretain, D.** (1987). Tridimensional architecture of the Golgi apparatus and its components in mucous cells of Brünner's glands of the mouse. *Am. J. Anat.* **179**, 95-107.
- Rambourg, A., Clermont, Y. and Képès, F.** (1993). Modulation of the Golgi apparatus in *Saccharomyces cerevisiae sec7* mutants as seen by three-dimensional electron microscopy. *Anat. Rec.* **237**, 441-452.
- Rambourg, A., Clermont, Y., Jackson, C. L. and Képès, F.** (1995a). Effects of brefeldin A on the three-dimensional structure of the Golgi apparatus in a sensitive strain of *Saccharomyces cerevisiae*. *Anat. Rec.* **241**, 1-9.
- Rambourg, A., Clermont, Y., Ovtracht, L. and Képès, F.** (1995b). Three-dimensional structure of tubular networks, presumably Golgi in nature, in various yeast strains: a comparative study. *Anat. Rec.* **243**, 283-293.
- Rossanese, O. W., Soderholm, J., Bevis, B. J., Sears, I. B., O'Connor, J., Williamson, E. K. and Glick, B. S.** (1999). Golgi structure correlates with transitional endoplasmic reticulum organization in *Pichia pastoris* and *Saccharomyces cerevisiae*. *J. Cell Biol.* **145**, 69-81.
- Rothman, J. E. and Wieland, F. T.** (1996). Protein sorting by transport vesicles. *Science* **272**, 227-234.
- Schekman, R.** (1992). Genetic and biochemical analysis of vesicular traffic in yeast. *Curr. Opin. Cell Biol.* **4**, 587-592.
- Thiéry, J. P. and Rambourg, A.** (1974). Cytochimie des polysaccharides. *J. Microsc. (Paris)* **21**, 225-232.